Journal of Sound and Vibration (1999) **221**(4), 587–606
Article No. jsvi.1998.2027, available online at http://www.idealibrary.com on IDEAL

IMPROVING THE PERFORMANCE OF A VIBRATION NEUTRALISER BY ACTIVELY REMOVING DAMPING

M. KIDNER AND M. J. BRENNAN
Institute of Sound and Vibration Research, University of Southampton, Highfield, Southampton SO17 1BJ, England

(*Received* 1 *April* 1998, *and in final form* 15 *October* 1998)

This paper describes the design of an active vibration neutraliser. The aim of the active element in the neutraliser is to reduce the internal damping of the device and thus make it more effective. Six different control configurations are considered and the input mechanical impedance of each configuration is calculated. This is used to assess the efficacy of each configuration. To study the behaviour of an active neutraliser a beam-like neutraliser is designed and built with piezoceramic patches providing the active element. An analytical model of this device is presented. Simulations and experimental results show that for two control configurations the amplitude of a mass-like structure with the neutraliser attached remains finite at a resonance of the composite system even when damping is entirely removed from the neutraliser, by the control system.

© 1999 Academic Press

1. INTRODUCTION

The vibration absorber was developed by Hartog and Ormonroyd at the beginning of the century [1]. It works on the principle of impedance mismatching. If a single-degree-of-freedom (SDoF), mass–spring–damper system is added to a vibrating system the impedance at the point of attachment becomes large at the natural frequency of the additional SDoF system. In this paper the additional system is referred to as a neutraliser, rather than an absorber. The reason for this is because the neutraliser works by the reaction force of the neutraliser mass equalling the force applied to the host structure, bringing it to rest; hence the term neutraliser. Alternatively it could be viewed as the energy from the structure being transferred into the motion of the mass of the neutraliser, hence the term absorber. What is fundamental, though, is that no energy is actually dissipated unless there is damping in the neutraliser. It is this damping that limits the behaviour of the neutraliser. This paper deals with the issue of using active control to reduce damping in the neutraliser thus improving its performance.

A neutraliser can be practically realised in a number of ways. Any resonant system, e.g., plates [2], beams [3] or pendulums [4] can be used. Snowdon *et al*.

0022–460X/99/040587 + 20 $30.00/0 © 1999 Academic Press

[3] used two beams in a cruciform to produce a neutraliser with two working frequencies. This allows for the suppression of the fundamental and another troublesome harmonic present in the host structures' vibration. It is a particularly elegant form of the neutraliser as it is mechanically very simple. Brennan [5] extended this design to incorporate ten cruciforms, each resonating at slightly different frequencies to produce a wide band neutraliser. The pendulum configuration was used in aircraft to reduce torsional oscillations in propeller shafts in 1935 [6]. It was developed later to be used in automotive engines, and was incorporated into the crank shaft. Sharif-Bakhtiar and Shaw [4] discuss the behaviour of the pendulum neutraliser with respect to its large amplitude non-linear oscillations and the effect of using stops to limit such behaviour. The attachment of a neutraliser, tuned to a structural resonance, reduces the motion of the structure at the tuned frequency and also produces a resonance on each side of the tuned frequency. If the frequency of excitation is not constant and drifts to the frequency of one of these resonances, large amplitudes will result. Semercigil *et al*. [7] propose the use of impact dampers to reduce the amplitude of these resonant peaks. Attached to the neutraliser mass it was found that they reduced amplitudes at the lower resonance significantly but only slightly at the upper resonance. When the neutraliser is tuned to suppress vibration at a frequency much higher than the structural resonance of a SDoF system, only one peak in the response is produced, which is above the tuned frequency. Brennan [8] has shown that the separation of the tuned frequency and this peak is a function of mass ratio (the ratio of the neutraliser mass to the mass of the structure). This paper shows that this peak can be limited to a finite value even when the damping is entirely removed from the neutraliser, by an active system.

As the neutraliser is only effective over a narrow frequency band, much research has gone into developing adaptive tuning systems. This accommodates varying forcing frequencies, caused for instance, by a change in running speed of a motor. An overview of such systems is given by von Flotow *et al*. [9]. The advantages of an actively tuned device is that low damping can be used if the tuning is precise, and this reduces the need for a large mass. There are many papers on different tuning methods, for example, Lai and Wang [10], Walsh and Lamancusa [11], Long *et al*. [12]. Few, however, have addressed the issue of counteracting the damping within the neutraliser as a means of improving performance. Olgac and Holm-Hansen [13] have approached the problem with the ''Delayed Resonator'', however the method involves the creation of an entirely active device, which although very adaptable, does not use the inherent passive properties of the neutraliser to their full effect.

Brennan [8] has shown that the effectiveness of the neutraliser is a function of the ratio of neutraliser and host structure impedances. For this reason the emphasis in this paper is placed on determining the input impedance of the active neutraliser. The improvement over the passive case can be determined by assessing the increase in impedance of the neutraliser and hence attenuation of the host structure, as a function of control gain. The control methods investigated in this paper look specifically at velocity feedback. The possibility of

combining velocity and displacement feedback to achieve both increased attenuation and tunability has yet to be addressed.

The paper is split into five sections. Following this introduction, section 2 develops the theory for a simple mass spring model of the neutraliser, and derives the input impedances of six possible neutraliser control arrangements. Three of these are selected for further study. The maxima and minima of the host structure's velocity with these three neutraliser configurations are studied as the feedback gain is increased. The third section develops an equivalent two-degree-of-freedom, mass–spring–damper system to model the behaviour of a beam vibrating in its first mode. Experimental results obtained from a beam-like neutraliser are presented in section 4 and finally, section 5 contains the conclusions.

2. COMPARISON OF ACTIVE NEUTRALISER CONFIGURATIONS

As described above the neutraliser is a SDoF system attached to a host structure. This can be represented by the system shown in Figure 1. The structure is considered as an impedance, Z_s at the point of attachment and the neutraliser is a simple mass–spring–damper configuration. Brennan [8] has shown that the attenuation of the vibration level of a *mass-like* host structure of mass m_s, at the neutraliser's tuned frequency and point of attachment, is a function of mass ratio and the damping.

$$\text{Atten} \approx \frac{\mu}{2\zeta}, \tag{1}$$

Where $\mu = m_n/m_s$ is the mass ratio and ζ is the damping ratio of the neutraliser.

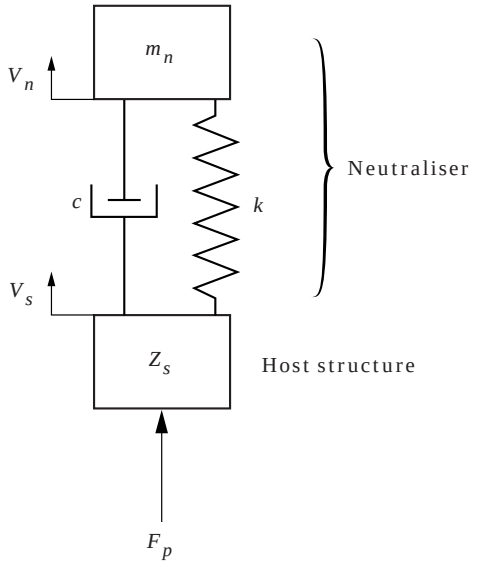

Figure 1. Assumed model of the neutraliser attached to a host structure of impedance Z_s. This model is used to calculate the response curve shown in Figure 2.

It can be seen from equation (1) that reduction of the damping ζ will increase the attenuation of the host structure's vibration.

The response of a mass-like host structure when a neutraliser is attached, is shown in Figure 2, for $\zeta = 0{\cdot}01 \rightarrow 0{\cdot}1$; in both cases the mass ratio $\mu = 0{\cdot}1$. This shows that the neutraliser works best when there is little damping in the system. The dip in the structural response is at the neutraliser's resonant frequency.

The purpose of the control system is to actively remove damping from the neutraliser by opposing any forces created by the inherent damping. This requires an actuator to be fitted to the neutraliser and/or host structure. An active neutraliser can be implemented in several ways, and in this section the differences between the control configurations are examined.

Because damping is proportional to velocity, the actuator can be fitted in a feedback loop where velocity is fed back with the appropriate gain g. Such a system is shown in Figure 3.

Six variations of the control scheme are possible. Either relative velocity across the spring, $(V_n - V_s)$, or absolute velocity, V_n, of the neutraliser is fed back. The control force can be applied either to the neutraliser mass, the host structure or between the neutraliser mass and the host structure. The following section considers which configuration is most advantageous.

2.1. INPUT IMPEDANCE

The input impedance of a neutraliser can be derived by combining the impedance of each element according to rules given in reference [14] and

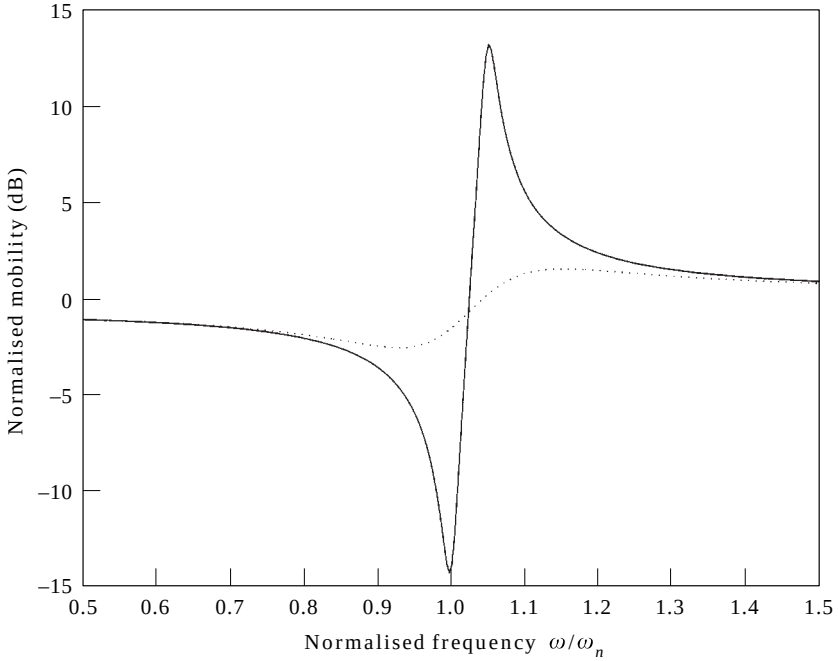

Figure 2. Host structure mobility (velocity/force) normalised to the mobility without a neutraliser attached. solid line: neutraliser has low damping, $\zeta = 0{\cdot}01$; dotted line: neutraliser has high damping, $\zeta = 0{\cdot}1$. ω_n is the tuned frequency of the neutraliser. Mass ratio, $\mu = 0{\cdot}1$.

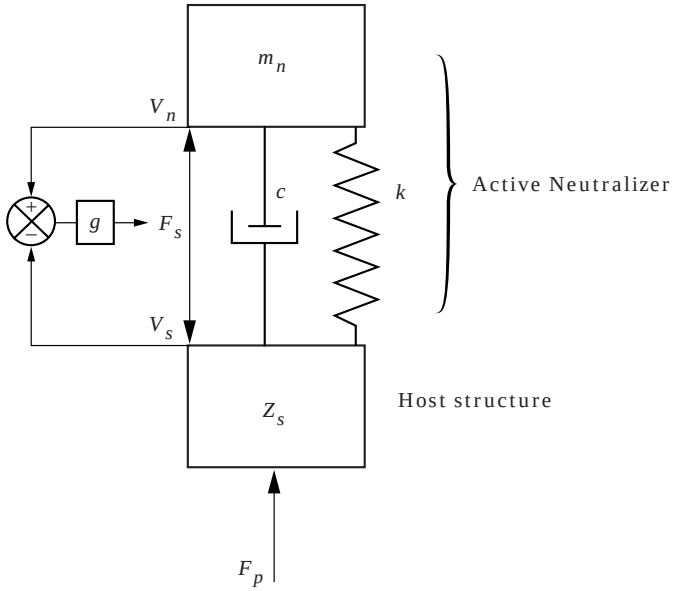

Figure 3. An active neutraliser attached to a host structure of impedance Z_s. g is a purely real gain.

considering the neutraliser in the way shown by Figure 4. Figure 4(a) shows a free body diagram of the neutraliser, which can then be considered as two impedances in series as shown in Figure 4(b). Z is the total impedance of the spring and damper given by $Z = Z_k + Z_c \equiv k/\mathrm{i}\omega + c$, and Z_m is the impedance of the neutraliser mass, given by $Z_m = \mathrm{i}\omega m$. The secondary forces, F_s can then be made to act on either of the impedances to model the control configurations. For instance, if it acts on both ends of the impedance Z it is equivalent to a force acting across the spring and damper of the neutraliser.

2.1.1. *Absolute velocity feedback*

Figure 4(b) shows the secondary force applied across the neutraliser spring. This is the most general case and is the arrangement for the actual neutraliser used in the experimental work in this paper. The other arrangements require independent locations for the secondary force to react from, which in practice would be an additional proof mass. The equations describing this system are

$$F_1 = ZV_1 - ZV_2 + F_s, \qquad F_2 = ZV_2 - ZV_1 - F_s, \qquad F_3 = Z_m V_3. \qquad (2\mathrm{a}-\mathrm{c})$$

Because we are considering absolute velocity feedback the secondary force F_s is given by gV_2, where g is the gain in the feedback loop.

By applying the boundary conditions of $F_2 = -V_3$ and $V_2 = V_3$, the resulting expression for the input impedance of the neutraliser, the ratio of F_1/V_1 is

$$Z_{AS} = \frac{ZZ_m}{Z_m + Z - g}. \qquad (3)$$

The subscript AS refers to absolute velocity feedback, with the force applied

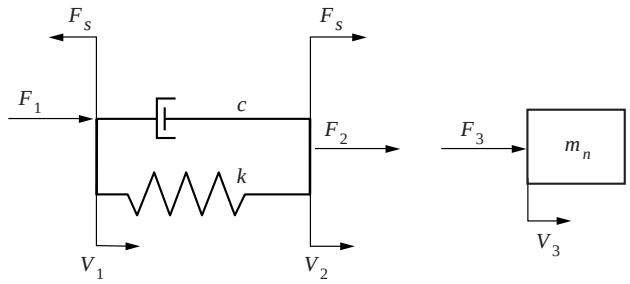

(a)

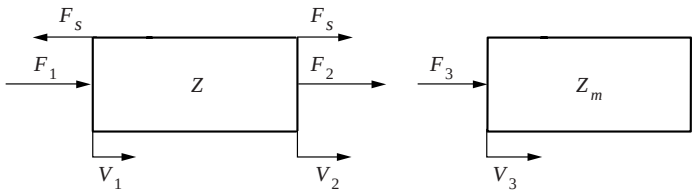

(b)

Figure 4. Analytical model of an active neutraliser. (a) Free body diagram; (b) impedance representation. $Z = Z_k + Z_c$.

across the spring of the neutraliser. When the neutraliser is tuned ($\omega = \omega_n$) the impedance reduces to

$$Z_{AS|\omega=\omega_n} = \frac{Z_m(Z_c - Z_m)}{Z_c - g} = \frac{\omega_n m(1 + 2\mathrm{i}\zeta)}{2(\zeta - \nu)} \tag{4}$$

where

$$\omega_n = \sqrt{\frac{k}{m}},\ \zeta = \frac{c}{2\omega_n m} \quad \text{and} \quad \nu = \frac{g}{2\omega_n m}$$

are the natural frequency of the neutraliser, the passive damping ratio of the neutraliser and the damping ratio due to the secondary force, respectively. It can be seen that the magnitude of the impedance at resonance is governed by the net damping ratio, when $\zeta = \nu$ the impedance becomes infinite.

From Figure 4 it can be seen that the two other cases can be derived by setting the secondary force on the mass or base to zero.

When the secondary force is applied only to the mass of the neutraliser, the three general equations describing the are again given by equations (2a–c). However, now the secondary force F_s in equation (2a) is set to zero. By solving the above equations as before an expression for the input impedance can be obtained.

$$Z_{AM} = \frac{F_1}{V_1} = \frac{Z(Z_m - g)}{Z_m + Z - g}. \tag{5}$$

The subscript AM refers to absolute velocity feedback when the force is applied to the neutraliser mass only. When $\omega = \omega_n$ this becomes

$$Z_{AM|\omega=\omega_n} = \frac{(Z_m - g)(Z_c - Z_m)}{Z_c - g} = \frac{\mathrm{i}\omega_n m(1 + 2\mathrm{i}\zeta)(1 + 2\mathrm{i}\omega_n^2\nu)}{2(\zeta - \nu)}. \tag{6}$$

The magnitude of the impedance when the neutraliser is tuned is governed by $\zeta - \nu$, so when the gain in the feedback loop is equal to the passive damping coefficient, $g = c$, the impedance becomes infinite.

The third case is that of the secondary force applied to the base of the neutraliser/host structure and being proportional to the absolute velocity of the neutraliser mass. Once again using the general equations shown in equation (2a–c), but setting the secondary force in equation (2b) to zero gives:

$$Z_{AB} = \frac{F_1}{V_1} = \frac{Z(Z_m - g)}{Z_m + Z}. \tag{7}$$

When $\omega = \omega_n$ this reduces to

$$Z_{AB|\omega=\omega_n} = \frac{(Z_m - g)(Z_c - Z_m)}{Z_c} = \frac{\mathrm{i}\omega_n m(1 + 2\mathrm{i}\zeta)(1 + 2\nu)}{2\mathrm{i}\zeta}. \tag{8}$$

It can be seen that when the neutraliser is tuned the magnitude of the impedance is primarily governed by the passive damping coefficient. This implies that the use of the active element does not improve upon the attenuation of the host structure achieved by the passive neutraliser.

2.1.2. *Relative velocity feedback*

In the configurations discussed in this section the feedback force is controlled by the relative velocity between the neutraliser mass and the host structure. This means that it behaves more like a conventional damper element. The arrangement is the same as that shown in Figure 4, except that the secondary force is now given by $F_s = g(V_2 - V_1)$. When the secondary force is placed across the spring it behaves like another damper whose sign and magnitude is controlled by the gain g. Following the procedure discussed in section 2.1.1 gives the input impedance,

$$Z_{RS} = \frac{Z_m(Z - g)}{Z_m + Z - g}, \tag{9}$$

where the subscript RS refers to relative velocity feedback applied across the neutraliser spring. When the neutraliser is tuned this reduces to an expression governed by the net damping in the neutraliser $\zeta - \nu$.

$$Z_{RS|\omega=\omega_n} = \frac{Z_m(Z_c - g - Z_m)}{Z_c - g} = \frac{\omega_n(1 + 2\mathrm{i}(\zeta - \nu))}{2(\zeta - \nu)}. \tag{10}$$

If the secondary force is applied to the mass the resulting input impedance is given by:

$$Z_{RM} = \frac{ZZ_m}{Z_m + Z - g}, \tag{11}$$

where the subscript RM refers to relative velocity feedback and the secondary force applied to the neutraliser mass only. It can be seen that equation (11) is the same as equation (3), so, when $\omega = \omega_n$ it reduces to equation (4).

In the final configuration considered in this paper, the secondary force is applied to the host structure/base of the neutraliser and is controlled by the relative velocity between the host structure and mass of the neutraliser, hence the subscript RB. In this case the input impedance is given by

$$Z_{RB} = \frac{Z_m(Z - g)}{Z_m + Z}. \tag{12}$$

When $\omega = \omega_n$ this reduces to

$$Z_{RB|\omega=\omega_n} = \frac{Z_m(Z_c - g - Z_m)}{Z_c} = \frac{\omega_n(1 + 2\mathrm{i}(\zeta - \nu))}{2\zeta}. \tag{13}$$

It can be seen from equation (13) that the magnitude of this impedance depends primarily on the passive damping.

All of the above results and the asymptotic behaviour of the expressions at frequencies, above, below and at the tuned frequency of the neutraliser are summarised in Table 1. At low frequencies the impedances tend to mass-like characteristics for all apart from Z_{AS} and Z_{AB}, which tend to $Z_m - g$. At high frequencies the impedances tend to the value of the damping element, Z_c apart from Z_{RS} and Z_{RB} where this is modified by the feedback gain to $Z_c - g$. For effective control the magnitude of the impedance at the tuned frequency must be dependent on g, as is the case when the secondary force is applied across the spring or to the neutraliser mass only. It should also be noted that applying forces to the neutraliser mass only is difficult to realise in practice as a proof mass is required.

2.2. IMPEDANCE MAXIMA AND MINIMA OF A HOST STRUCTURE WITH A NEUTRALISER ATTACHED

The main objective of an active neutraliser is to increase the attenuation in vibration of the host structure at the neutraliser's tuned frequency. However, the presence of the neutraliser also produces a combined host structure and neutraliser resonance at a frequency above the tuned frequency of the neutraliser. In this section the magnitudes of the maxima and minima of the combined impedance are considered. The maxima and minima in impedance correspond to dips and peaks in the response of the host structure. As the impedance for relative velocity feedback with the force applied to the mass, and absolute velocity with the force applied across the spring are the same, we shall consider only three cases, Z_{AS}, Z_{RS} and Z_{AM}. It is also assumed that the excitation frequency is such that the host structure is mass-like at this frequency.

TABLE 1

Summary of input impedances to neutraliser configurations

	Impedance	Impedance at the tuned frequency	Impedance as $\omega \Rightarrow 0$	Impedance as $\omega \Rightarrow \infty$
Absolute feedback				
Force across spring	$Z_{AS} = \dfrac{Z_m Z}{Z_m + Z - g}$	$\dfrac{Z_m(Z_c - Z_m)}{Z_c - g}$	Z_m	Z_c
Force on mass	$Z_{AM} = \dfrac{(Z_m - g)Z}{Z_m + Z - g}$	$\dfrac{(Z_m - g)(Z_c - Z_m)}{Z_c - g}$	$Z_m - g$	Z_c
Force on base	$Z_{AB} = \dfrac{(Z_m - g)Z}{Z_m + Z}$	$\dfrac{(Z_m - g)(Z_c - Z_m)}{Z_c}$	$Z_m - g$	Z_c
Relative feedback				
Force across spring	$Z_{RS} = \dfrac{Z_m(Z - g)}{Z_m + Z - g}$	$\dfrac{Z_m(Z_c - g - Z_m)}{Z_c - g}$	Z_m	$Z_c - g$
Force on mass	$Z_{RM} = \dfrac{Z_m Z}{Z_m + Z - g}$	$\dfrac{Z_m(Z_c - Z_m)}{Z_c - g}$	Z_m	Z_c
Force on base	$Z_{RB} = \dfrac{Z_m(Z - g)}{Z_m + Z}$	$\dfrac{Z_m(Z_c - g - Z_m)}{Z_c}$	Z_m	$Z_c - g$

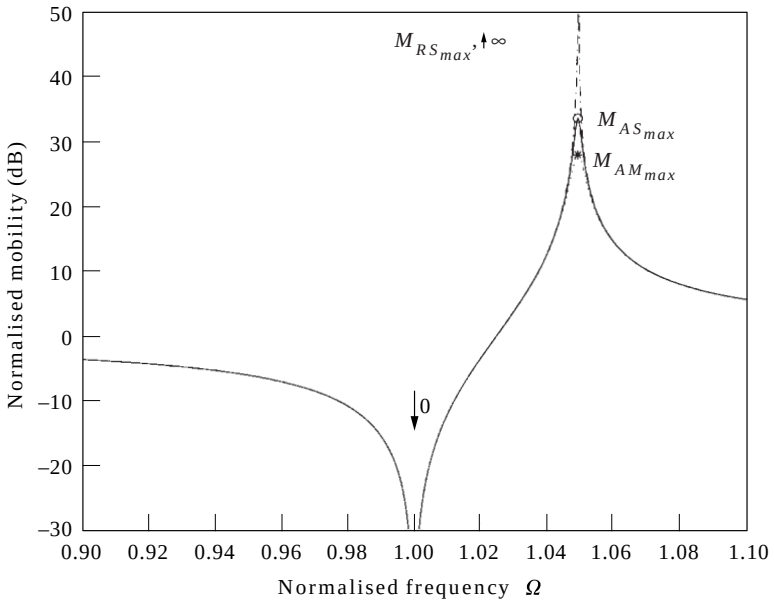

Figure 5. Host structure mobility normalised to the mobility without a neutraliser attached for the three control configurations. M_{RS} (dash-dot line): relative velocity feedback with the force applied across the spring; M_{AS} (solid line): absolute velocity feedback with the force applied across the spring; M_{AM} (dotted line): absolute velocity feedback with the force applied to the neutraliser mass. The *max* values ○, * correspond to the minimum impedance expressions shown in equations (17) and (20), respectively. Note that all the response curves go to $-\infty$ at the tuned frequency. $g = c$, $\zeta = 0{\cdot}01$, mass ratio $\mu = 0{\cdot}1$.

This allows the impedance of the host structure to be simplified to that of a mass, m_s.

When the control force governed by the relative velocity is applied across the neutraliser spring, and the gain is equal to the damping coefficient, the effect is to remove the damping from the system. This sets the response of the host structure to zero at the working frequency of the neutraliser but results in an infinite response at the adjacent resonance which can be seen by examining Figure 5. To compare the benefits of the other feedback strategies with this case, the response of the host structure at this resonance frequency is examined for a gain setting of $Z_c = g$.

If the Z_{AS} configuration, (absolute velocity feedback with the control force across the spring), is considered, the input impedance (F_p/V_s) of the system shown in Figure 1 is given by

$$Z_{t_{AS}} = Z_s + Z_{AS}, \tag{14}$$

where Z_s is the impedance of the host structure. Substitution of the expression for Z_{AS} given in Table 1 results in:

$$Z_{t_{AS}} = \frac{Z_m Z + Z_s(Z_m + Z - g)}{Z_m + Z - g}. \tag{15}$$

Now, it has been shown by Brennan [8] that the resonance frequency ($\omega = \omega_s$)

occurs when

$$Z_k = \frac{-Z_s Z_m}{Z_m + Z_s}. \tag{16}$$

Substituting from equation (16) into equation (15) one can evaluate the minima in the impedance. By setting $g = Z_c$, gives

$$Z_{t_{AS}|_{\substack{\omega=\omega_s \\ g=Z_c}}} = Z_c\left(1 + \frac{1}{\mu}\right). \tag{17}$$

This is the minimum value of the input impedance of the system, which corresponds to the maximum response of the host structure. This is shown by the point $M_{AS_{\max}}$ in Figure 5. The solid line in Figure 5 illustrates the mobility of the host structure when $g = c$ and absolute velocity feedback controls the force applied across the spring of the neutraliser. This shows that $g = Z_c$ does not produce an infinite response at the resonance of the complete system. For comparison, Z_{RS}, (relative velocity feedback with the secondary force applied across the neutraliser spring) is zero for this condition, which means the host structure response is infinite at the resonant frequency

When the secondary force is proportional to the absolute velocity of the neutraliser mass and is applied only to the neutraliser mass the total impedance of the system (shown in Figure 1) is given by

$$Z_{t_{AM}} = Z_{AM} + Z_s. \tag{18}$$

Substuting for Z_{AM} given in Table 1 and combining this with equation (16) gives, after setting $g = Z_c$ the minima in the impedance.

$$Z_{t_{AM}|_{\substack{\omega=\omega_s \\ g=Z_c}}} = \frac{Z_c(Z_m(Z_m + 2Z_s) - Z_c(Z_m + Z_s))}{Z_m^2}. \tag{19}$$

If $Z_s \gg Z_m$, i.e., $\mu \ll 1$, and $\zeta \ll 1$ as is often the case in practice, then equation (19) becomes.

$$Z_{t_{AM}|_{\substack{\omega=\omega_s \\ g=Z_c}}} = \frac{2Z_c}{\mu}. \tag{20}$$

This is the minimum value of the input impedance of the system, which corresponds to the maximum response. This again shows that $g = Z_c$ does not produce an infinite response at the resonance frequency, as shown by the point $M_{AM_{\max}}$ in Figure 5. By taking the ratio of equation (20) to equation (17) the reduction of vibration level at the complete systems resonance due to adopting AM control over AS control can be quantified as:

$$\frac{Z_{t_{AM}|_{\substack{\omega=\omega_s \\ g=Z_c}}}}{Z_{t_{AS}|_{\substack{\omega=\omega_s \\ g=Z_c}}}} = \frac{1 + \mu}{2}. \tag{21}$$

By applying the condition $\mu \ll 1$, equation (21) tends to $\frac{1}{2}$. This means the vibration level at the resonance frequency when adopting AM control is 6 dB

lower than when AS control is used. This advantage has to be balanced against the practical difficulties of applying a secondary force to the neutraliser mass only.

The previous analysis shows that for the AM and AS control configurations the amplitude at the complete structure resonance does not become infinite when $g = Z_c$. To calculate the gain at which the response at this resonance does become infinite we can set the numerator of the impedance expression to zero and solve for g. The resulting value of g is termed the critical gain and for the AS control configuration is given by

$$g_{c_{AS}} = \frac{Z_m Z + Z_s(Z_m + Z)}{Z_s}, \tag{22}$$

which can be evaluated at the resonance frequency by substituting for Z_k from equation (16). This results in

$$g_{c_{AS}|\omega=\omega_s} = Z_c(\mu + 1). \tag{23}$$

When the secondary force is applied to the neutraliser mass only, e.g., the AM control configuration, the critical gain is given by

$$g_{c_{AM}} = \frac{Z_m Z + Z_s(Z_m + Z)}{Z_s + Z}. \tag{24}$$

At the resonance frequency this becomes

$$g_{c_{AM}|\omega=\omega_s} = Z_c(1 + \mu)^2. \tag{25}$$

In both Z_{AM} and Z_{AS} cases, provided that $\zeta \ll 1$ and $\mu \ll 1$, so that $Z_s \gg Z_c$, the critical gain is a function of the mass ratio μ. This is illustrated in Figure 6(a) which shows the velocity of the host structure under control at the resonance frequency normalised to the passive case. It shows that the for the absolute velocity feedback control configurations the response does not become very large until the gain is greater than the passive damping coefficient of the neutraliser. This also means that the condition $g = c$, which reduces the vibration of the host structure at $\omega = \omega_n$ to zero, can be reached under broadband excitation without causing instability at ω_s. Figure 6(b) shows how the dip in response at the tuned frequency varies with control gain for the three different configurations. It can be seen that all three configurations are equally effective at the tuned frequency.

3. ANALYTICAL MODEL OF A BEAM-LIKE NEUTRALISER

The active neutraliser used for the experimental work in this paper takes the form of a double cantilever beam, a schematic of which is shown in Figure 7(a). Note that this is also equivalent to a free–free beam with a force acting at it's centre point. The secondary force is provided by the two moments applied at a distance d_p from the centre of the beam, (these moments are generated by a piezo-ceramic patch glued to the beam). The centre point is the point of attachment to the host structure. This section shows that the beam-like

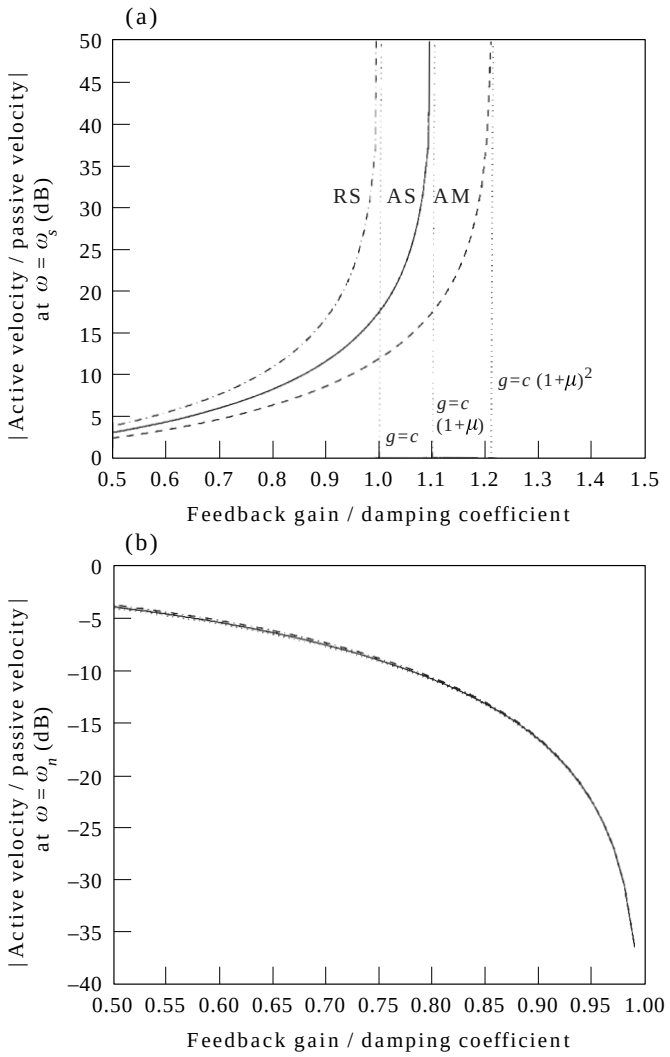

Figure 6. (a) Velocity of the host structure for three control configurations, at (a) $\omega = \omega_s$, and (b) $\omega = \omega_n$ normalised to the passive velocity versus the feedback gain; $\mu = 0{\cdot}1$. M_{RS} (dash-dot line): relative velocity feedback with the force applied across the spring; M_{AS} (solid line): absolute velocity feedback with the force applied across the spring; M_{AM} (dashed line): absolute velocity feedback with the force applied to the neutraliser mass.

neutraliser can be approximated by the system shown in Figure 7(b). This is similar to the neutraliser discussed in the previous section, but with the addition of a mass m_1. Conceptually m_1 can be attached to the host structure, leaving a system which is identical to the neutraliser discussed previously, (damping is neglected for clarity). The aim of this section is to relate the secondary force, F_s, the stiffness of the neutraliser spring, k and the neutraliser mass, m_2 to the applied moments, M and the material properties of the beam. To develop this equivalent two-degree-of-freedom (2DoF) system the point impedances ($F_p/V(0)$, F_p/V_1) and transfer impedances, (M/V (0), F_s/V_1) of the beam and the SDoF model respectively must be considered.

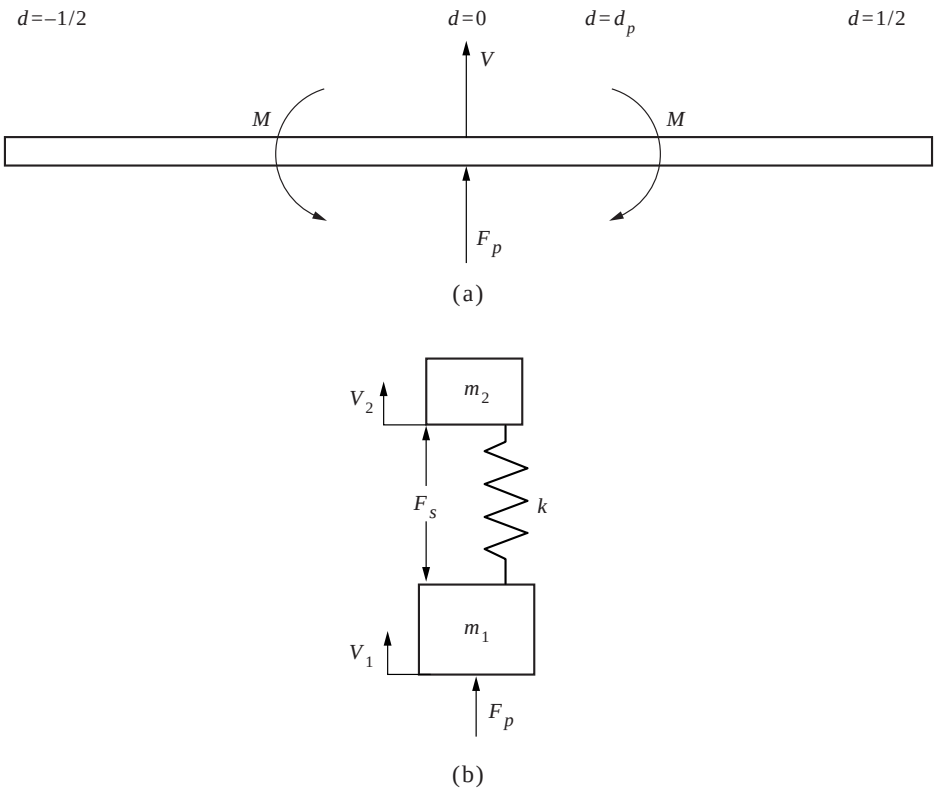

Figure 7. (a) Idealization of free–free beam used in experimental work. F_p is the excitation force and M are moments provided by the piezo ceramic element. (b) Basic two-degree-of-freedom model of a beam-like neutraliser.

3.1. RESPONSE TO A POINT FORCE

If an undamped free–free beam is considered as in Figure 7(a) the point force mobility can be written as the summation over all the modes of vibration [15].

$$\frac{V(0)}{F_p(0)} = \frac{1}{\mathrm{i}\omega m_T} + \sum_{r=1}^{\infty} \frac{\mathrm{i}\omega\phi_r^2(0)}{m_T(\omega_r^2 - \omega^2)}, \tag{26}$$

Where $\phi_r(0)$ is the rth mode shape of a free–free beam at $d=0$, m_T is the total mass of the beam and ω_r is the resonant frequency of the rth mode. The main assumption in the development of this equivalent model is that higher order modes do not significantly contribute to the dynamic response in the frequency range of interest

Because of this, only the rigid body mode and first mode of vibration are considered, so the mobility can be written as

$$\frac{V(0)}{F_p(0)} = \frac{1}{\mathrm{i}\omega m_T} + \frac{\mathrm{i}\omega\phi_1^2(0)}{m_T(\omega_1^2 - \omega^2)}. \tag{27}$$

This can be rearranged to give the impedance

$$\frac{F_p(0)}{V(0)} = \frac{\mathrm{i}\omega m_T(\omega_1^2 - \omega^2)}{\omega_1^2 - \omega^2(1 + \phi_1^2(0))}. \tag{28}$$

Inspection of equation (28) shows that the beam impedance is zero at $\omega = \omega_1$, the first resonance of the beam, and is infinite when

$$\omega^2 = \omega_a^2 = \frac{\omega_1^2}{1 + \phi_1^2(0)}, \tag{29}$$

the first anti-resonance of the beam.

Now consider the two-degree-of-freedom system shown in Figure 7(b). The impedance of the system is given by:

$$\frac{F_p}{V_1} = \mathrm{i}\omega \frac{\left(\dfrac{m_1 + m_2}{m_1}\right)\omega_n^2 - \omega^2}{\dfrac{1}{m_1}(\omega_n^2 - \omega^2)}, \tag{30}$$

where $\omega_n = \sqrt{k/m_2}$. This is infinite when $\omega = \omega_n$ and zero when

$$\omega = \omega_m = \sqrt{\omega_n^2 \frac{m_1 + m_2}{m_1}}. \tag{31}$$

Setting $\omega_a = \omega_n$, i.e., equating the frequencies at which the point impedance of the beam and the impedance of the equivalent 2DoF system are both zero, gives

$$\omega_1^2 \frac{1}{1 + \phi_1(0)^2} = \omega_m^2 \frac{m_1}{m_1 + m_2}. \tag{32}$$

Setting $\omega_1 = \omega_m$, i.e., equating the frequencies at which the point impedance of the beam and the impedance of the equivalent 2DoF system are both infinite, then one gets a relationship between the ratio of the masses m_2/m_1 and the square of the mode shape evaluated at the centre of the beam i.e.,

$$\frac{m_2}{m_1} = \phi_1^2(0) = 1{\cdot}478. \tag{33}$$

Hence, the equivalent mass–spring system has masses in the following ratio $m_2 = 0{\cdot}596 m_T$, where m_T is the total mass of the beam. This means that only 0·596 of the beam mass is effective in the beam-like neutraliser, the remaining $0{\cdot}404 m_T$ is effectively added to the mass of the host structure.

3.2. RESPONSE DUE TO THE PIEZO-CERAMIC ELEMENTS

The development of an equivalent system for moment excitation is fundamental in successfully modelling the active control of the neutraliser in a simple 2DoF form. Consider the moments applied in Figure 7(a), the general form of the velocity response at $d = 0$ to a single moment at $d = d_p$ is given by [15]

$$\frac{V(0)}{M(d_p)} = \sum_{r=1}^{\infty} \left(\frac{\mathrm{i}\omega \phi_r'(d_p)\phi_r(0)}{m_T(\omega_1^2 - \omega^2)} \right), \tag{34}$$

where $\phi_r'(d_p)$ is the spatial derivative of the mode shape at $d = d_p$, and $\phi_r(0)$ is the mode shape at $d = 0$. In the case illustrated in Figure 7(a) the excitation is symmetrical about $d = 0$. By considering only the first bending mode and noting that the beam is being excited by two moments $M(d_p)$ equation (34) can be written as

$$\frac{2\mathrm{i}\omega M(d_p)\phi_1'(d_p)\phi_1(0)}{m_T\omega_1^2 V(0)} = \frac{\omega^2}{\omega_1^2} - 1. \tag{35}$$

If a mass–spring system as shown in Figure 7(b) is considered, the transfer impedance between the secondary force and the velocity V_1 is

$$\frac{F_s}{V_1} = \frac{-\omega^2 m_1 + \omega_n^2(m_1 + m_2)}{\mathrm{i}\omega}. \tag{36}$$

Where $\omega_n^2 = k/m_2$. Noting that $\omega_1 = \omega_m$ this can be rearranged to give

$$\frac{F_s}{V_1} = -\frac{m_T\omega_n^2}{\mathrm{i}\omega}\left(\frac{\omega^2}{\omega_1^2} - 1 \right). \tag{37}$$

Setting

$$\omega_n^2 = \frac{\omega_1^2}{1 + \phi^2(0)}$$

as before and rearranging yields,

$$\frac{\mathrm{i}\omega F_s(1 + \phi_1^2(0))}{V_1 m_T \omega_1^2} = \frac{\omega^2}{\omega_1^2} - 1. \tag{38}$$

Setting equation (38) equal to equation (35) yields the relationship between a moment applied to a beam and the secondary force in the simple mass–spring system.

$$F_s = -\left(\frac{2\phi'(d_p)\phi_1(0)}{1 + \phi_1(0)^2} \right) M. \tag{39}$$

Noting that the derivative of the mode shape $\phi'(d_p)$ is proportional to the flexural wave number k, which is in turn proportional to the square root of frequency, means that the equivalent secondary force in the 2DoF model has a frequency dependance, i.e., $F_s/M \propto \omega_r^{1/2}$. This means that if the beam-like neutraliser is tuned to a high frequency, i.e., has a short beam length, the secondary force will be very effectively produced by applying a moment to the beam. However, at a low tuned frequency, i.e., long beam length, the secondary force will be much smaller.

The above analysis shows that an equivalent 2DoF system can be developed for a beam-like neutraliser, by dividing the total mass of the beam into two masses as a function of the mode shape of the fundamental frequency of a free–free beam. It has also shown that moments applied to a beam and the secondary forces acting on the 2DoF system are related by a function of mode shape and it's spatial derivative.

4. EXPERIMENTAL WORK

The neutraliser discussed in section 3 was physically realised as a perspex beam ($6 \times 40 \times 200$ mm) with two piezo-ceramic (PZT) actuators ($0{\cdot}5 \times 31 \times 40$ mm) symmetrically attached to the top surface, as shown in Figure 8, to generate the moments M [16]. Perspex was used because it has high internal damping allowing any improvements due to active control to be easily measured and reducing the dynamic range of the measurements. The purpose of the experimentation was to verify the predicted active and passive impedances.

Figure 8 shows the experimental set-up used to measure the point mobility of the beam. A Hewlett Packard 3567/A analyser produced a narrow band ($200 \rightarrow 400$ Hz) random excitation signal used to drive an electro-dynamic shaker attached to the centre point of the beam. The applied force was measured directly using a B&K force gauge (type 8200), and acceleration at the centre and end points of the beam was also measured. These acceleration signals were intergrated using the B&K charge amplifiers (type 2635) to give the velocities. The relative velocity between the end and centre of the beam was passed through

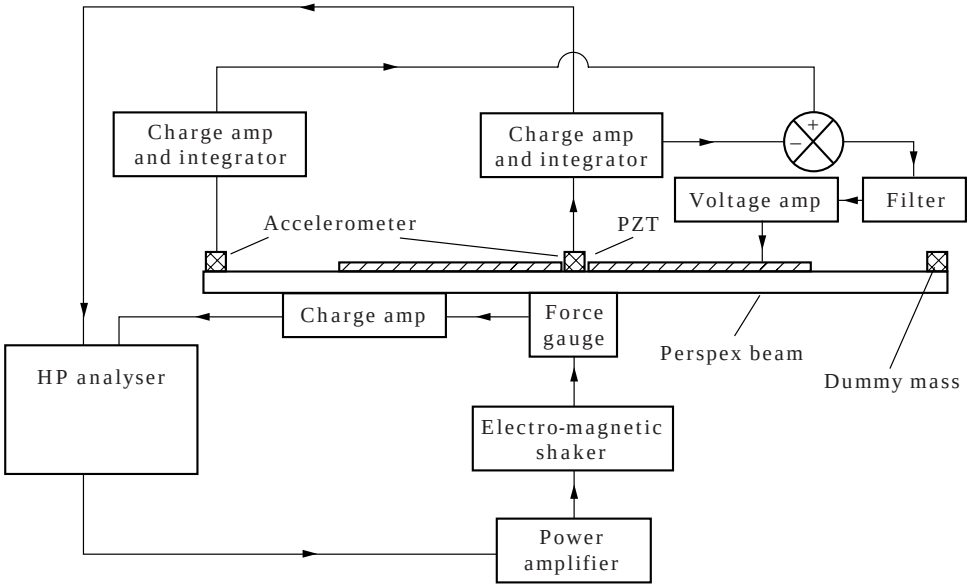

Figure 8. Diagram of the experimental set-up to measure the mobilities of AS (absolute velocity feedback with the force applied across the spring), and RS (relative velocity feedback with the force applied across the spring), control configurations.

a low pass filter, with a -3 dB cut-off point at 1 kHz, and was subsequently fed into a B&K power amp type 2713 to control the PZT actuators. The point mobility was then measured over the frequency range of $200 \rightarrow 400$ Hz, and the feedback gain was set so that $g \approx c$. Setting the gain exactly equal to the damping coefficient c was not possible as the system would become unstable. The mobility with absolute velocity feedback employed was then measured. In both cases the secondary force was effectively acting across the neutraliser spring. The results are shown in Figure 9.

Figure 9 also shows the theoretical mobility, using the equivalent 2DoF system developed in section 3. For the theoretical results the gain was set such that $g = 0{\cdot}9c$. The passive damping was measured by matching the phase response of a dynamic stiffness model of the beam to the phase of the measured passive mobility. The equivalent masses were calculated in accordance with the method shown in section 3. The smaller amplitude at the resonance frequency, about 308 Hz, in Figure 9(a) compared with Figure 9(b), suggests that absolute velocity feedback with the secondary force applied across the spring of the neutraliser is the preferred method of control. It also has practical advantages because it only requires one velocity to be measured.

The agreement between the experiment and the equivalent 2DoF system is considered to be reasonably good, and hence validates the theorectical models developed in sections 2 and 3.

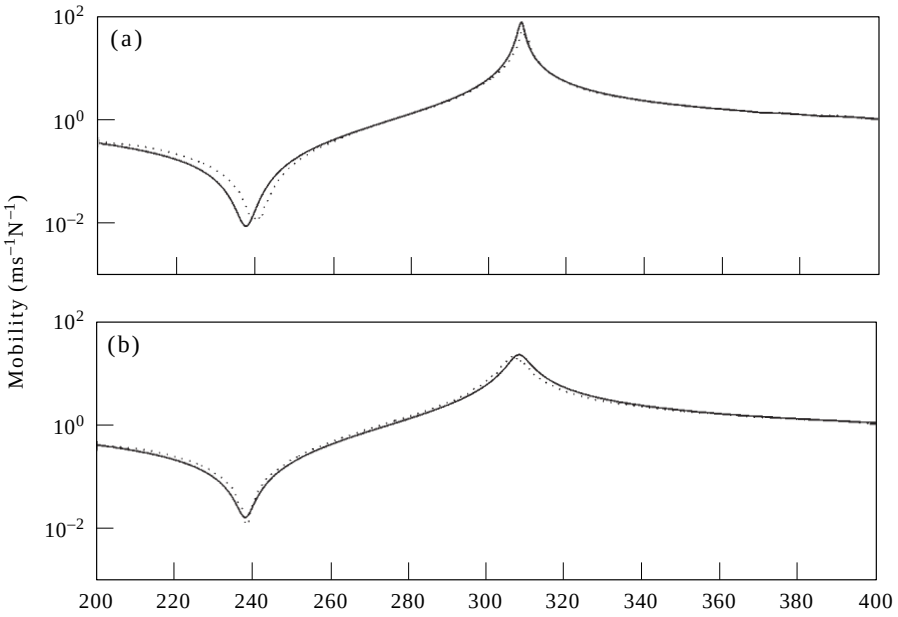

Figure 9. Comparison of experimental and theorectical plots for mobility. (a) RS, relative velocity feedback with the force applied across the spring. (b) AS, absolute velocity feedback with the force applied across the spring. Solid line: model; dotted: experimental data. For models, $g = 0{\cdot}9c$, $\zeta = 0{\cdot}0311$ and $\mu = 0{\cdot}67$.

5. CONCLUSIONS

This paper has presented an active control method for reducing the damping in a vibration neutraliser, hence increasing the attenuation of the host structure that it can provide at the point of attachment. It has been shown that the use of absolute velocity feedback has distinct advantages over the use of relative velocity feedback. The most important of which is achieving a finite amplitude at the complete system resonance, whilst still obtaining maximum attenuation at the working frequency of the neutraliser.

An equivalent 2DoF model of a beam has been developed and shown to accurately model the dynamics of a beam-like neutraliser. This greatly simplifies the analysis of beam-like neutralisers.

Experimental results agree with the predictions from the 2DoF model and show that using a secondary force to remove damping is a valid method of improving the performance of vibration neutralisers. This, combined with active tuning technology, has the potential to produce a very versatile vibration control device.

REFERENCES

1. J. D. Hartog and J. Ormonroyd 1928 *Transactions of the ASME*, **APM5O-7**, 11–22. Theory of the dynamic absorber.
2. J. Clemens 1984 *Journal of the Acoustical Society of America* **75**, 638. Plate like dynamic absorbers – comparison of measurement and theory.
3. J. Snowdon, A. Wolfe and R. Kerlin 1984 *Journal of the Acoustical Society of America*. **75**, 1792–1799. The cruciform dynamic absorber.
4. M. Sharif Bakhtiar and S. Shaw 1988 *Journal of Sound Vibration* **126**, 221–235. The dynamic response of a centrifugal pendulum vibration absorber with motion limiting stops.
5. M. J. Brennan 1997 *Noise Control Engineering Journal*. **45**, 201–207, Characteristics of a wideband vibration neutraliser.
6. C. Taylor 1970 The Internal Combustion Engine in Theory and Practice, Volume 2 (Combustion Fuels, Materials, Design). Cambridge, MA: MIT Press.
7. S. Semercigil, D. Lammers and Z. Ying, 1992 *Journal of Sound and Vibration* **156**, 445–459. A new tuned vibration absorber for wide band excitation.
8. M. Brennan 1997 *Proceedings of the Institute of Mechanical Engineers* **211** (part C), 91–108, Vibration control using a tunable vibration neutraliser.
9. A. H. von Flotow, A. Beard and D. Bailey 1994 in *Noise Con* 94. **1**, 437–454. Adaptive tuned vibration absorbers: tuning laws, tracking agility, sizing and physical implementations.
10. J. S. Lai and K. W. Wang 1996 *Journal of Vibration and Acoustics*. **118**, 41–47. Parametric control of structural vibrations via adaptable stiffness dynamic absorbers.
11. P. Walsh and J. Lamancusa 1992 *Journal of Sound and Vibration* **158**, 195–211. A variable stiffness vibration absorber for the minimization of transient vibration.
12. T. Long, M. Brennan and S. Elliott 1997 *Proceedings of the Institute of Mechanical Engineers Part I*, **12**, 215–228. Design of smart machinery installations to reduce transmitted vibrations by adaptive modificatations of internal forces.
13. N. Olgac and B. Holm-Hansen 1994 *Journal of Sound and Vibration* **176**, 93–104. A novel active vibration absorber technique: delayed resonator.
14. V. H. Neubert 1987 *Mechanical Impedance: Modelling/Analysis of Structures*. Department of Engineering and Mechanics, Pennsylvania State University.

15. R. E. D. BISHOP and D. C. JOHNSON 1960 *The Mechanics of Vibration*, Cambridge University Press.
16. M. J. BRENNAN, M. J. DAY, S. J. ELLIOTT and R. J. PINNINGTON 1994 in *IUTAM* **94**, 263–274. Piezoelectric actuators and sensors.